Journal of Neurochemistry

JNC

JOURNAL OF NEUROCHEMISTRY | 2020 | 152 | 468–481

doi: 10.1111/jnc.14891

ORIGINAL ARTICLE

A multimolecular signaling complex including PrP^C and LRP1 is strictly dependent on lipid rafts and is essential for the function of tissue plasminogen activator

Vincenzo Mattei*†,[1], Valeria Manganelli†,[1], Stefano Martellucci*†, Antonella Capozzi†, Elisabetta Mantuano†‡, Agostina Longo†, Alberto Ferri§¶, Tina Garofalo†, Maurizio Sorice† and Roberta Misasi†

*Biomedicine and Advanced Technologies Rieti Center, Sabina Universitas, Rieti, Italy

†Department of Experimental Medicine, Sapienza University, Rome, Italy

‡Department of Pathology, University of California at San Diego, La Jolla, CA, USA

§Institute of Cell Biology and Neurobiology, CNR, Rome, Italy

¶Fondazione Santa Lucia IRCCS, c/o CERC, Rome, Italy

Abstract

Prion protein (PrP^C) localizes stably in lipid rafts microdomains and is able to recruit downstream signal transduction pathways by the interaction with promiscuous partners. Other proteins have the ability to occasionally be recruited to these specialized membrane areas, within multimolecular complexes. Among these, we highlight the presence of the low-density lipoprotein receptor-related protein 1 (LRP1), which was found localized transiently in lipid rafts, suggesting a different function of this receptor that through lipid raft becomes able to activate a signal transduction pathway triggered by specific ligands, including Tissue plasminogen activator (tPA). Since it has been reported that PrP^C participates in the tPA-mediated plasminogen activation, in this study, we describe the role of lipid rafts in the recruitment and activation of downstream signal transduction pathways mediated by the interaction among tPA, PrP^C and LRP1 in human neuroblastoma SK-N-BE2 cell line. Co-immunoprecipitation analysis reveals a consistent association between PrP^C and GM1, as well as between LRP1 and GM1, indicating the existence of a glycosphingolipid-enriched multimolecular complex. In our cell model, knocking-down PrP^C by siRNA impairs ERK phosphorylation induced by tPA. Moreover the alteration of the lipidic milieu of lipid rafts, perturbing the physical/functional interaction between PrP^C and LRP1, inhibits this response. We show that LRP1 and PrP^C, following tPA stimulation, may function as a system associated with lipid rafts, involved in receptor-mediated neuritogenic pathway. We suggest this as a multimolecular signaling complex, whose activity depends strictly on the integrity of lipid raft and is involved in the neuritogenic signaling.

Keywords: GM1, lipid rafts, LRP1, methyl-β-cyclodextrin, prion protein, tPA.

J. Neurochem. (2020) **152**, 468–481.

In analogy with many other GPI-anchored proteins, the cellular prion protein (PrP^C) localizes in lipid rafts microdomains (Taylor and Hooper 2006; Mattei *et al.*, 2015) and over the past fifteen years, evidence has accumulated that PrP^C can act as a cell surface receptor, co-receptor or ligand, able to recruit downstream signal transduction pathways

Received June 7, 2019; revised manuscript received October 4, 2019; accepted October 7, 2019.

Address correspondence and reprint requests to Roberta Misasi, Dip. Medicina Sperimentale, "Sapienza" University of Rome, Viale Regina Elena, 324, 00161 Rome, Italy. E-mail: roberta.misasi@uniroma1.it

[1]These authors contributed equally to this work.

Abbreviations used: DMEM, Dulbecco's Modified Eagle Medium; FCS, fetal calf serum; FB1, fumonisin B1; LRP1, low-density lipoprotein receptor-related protein 1; mAb, monoclonal antibody; MβCD, methyl-β-cyclodextrin; NMDA-R, N-methyl-D-aspartate receptor; pAb, polyclonal Antibody; PrP^C, Prion protein; PVDF, polyvinylidene difluoride; SDS-PAGE, sodium dodecyl sulphate–polyacrylamide gel electrophoresis; siRNA, small interfering RNA; tPA, tissue plasminogen activator.

(Martellucci *et al.,* 2018; Martellucci *et al.,* 2019). Such function is thought to be driven by the interaction of PrP^C with promiscuous partners, within multimolecular complexes (Hirsch *et al.,* 2014). Lipid rafts are a dynamic assemblage of sphingolipids, cholesterol and proteins that dissociate and associate rapidly forming functional clusters in cell membranes (Sorice *et al.,* 2009; Sonnino, 2012). These clusters provide highly efficient lipid–protein modules, which operate in membrane trafficking and cell signaling (Sorice *et al.,* 2010). Indeed, lipid rafts are thought to function as platforms that sequestrate specific proteins, permanently or transiently, thus introducing and modulating cell signaling (Mattei *et al.,* 2017). The combinatorial possibilities offered by the wide range of lipid isoforms, glycan structures, and actin dynamics, confers an extraordinary assortment of possibilities for receptor clustering, endocytosis and signaling at the plasma membrane (Gonnord and Blouin, 2012). Considered the fluidity and plasticity of lipid rafts, some proteins are transiently recruited to these specialized membrane areas to form the functional receptor clustering and among these MACROBUTTON HTMLDirect is to highlight the presence of the low-density lipoprotein receptor-related protein 1 (LRP1) (Wu 2005; Sorice *et al.,* 2008; Roura *et al.,* 2014). LRP1 is a membrane-associated protein (~600 kDa) that is nicked during biosynthesis to give two stably associated polypeptides: an 85-kDa membrane-spanning C-terminal fragment and a 515-kDa extracellular N-terminal chain. LRP1 is expressed amply on neurons (Bu *et al.,* 1994), (Moestrup and Gliemann, 1992), where its fundamental role is the uptake of glial-derived sterol and lipid required for membranes and synapse formation (Mauch *et al.,* 2001). In addition, LRP1 binds to more than 30 extracellular ligands, and its cytoplasmic domain binds to endocytic and scaffold adaptors that link the receptor to other membrane proteins (Zerbinatti *et al.,* 2004; Herz and Chen 2006). Furthermore, LRP1 was previously identified as receptor partner of PrP^C that is able to regulate its internalization. Indeed, LRP1 is required for the Cu^{2+}-dependent endocytosis of exogenous PrP^C on neuronal cells (Taylor and Hooper, 2007; Parkyn *et al.,* 2008). The role of LRP1 as endocytic molecule has been first described (Strickland and Gonias, 2002; Zemskov *et al.,* 2007; Gonias and Campana, 2014), subsequently ourselves and other authors showed the role of LRP1 as cell signaling receptor in response to specific ligands (Sorice *et al.,* 2008; Gonias and Campana, 2014).

While for the function of the endocytic receptor, the distribution of LRP1 on the plasma membrane is external to the lipid rafts, to perform the signal function LRP1 is temporarily recruited in lipid microdomain, in fact the breakdown of the raft considerably alters the signaling function induced by LRP1 ligands, including tissue plasminogen activator (tPA) and the resulting neurotrophic function (Laudati *et al.,* 2016), while it does not affect endocytic function (Gonias and Campana, 2014). This particular ability of LRP1 to locate inside or outside lipid rafts, depending on the activity, gives to this molecule a greater interest as a multifunction receptor that can form multimolecular complexes with independently regulated functions. Indeed, the interaction with different co-receptors seems to be necessary for LRP1 to play its functions and therefore the LRP1-dependent activation of specific cell signaling is not ubiquitous in all cells and tissues in which LRP1 is expressed, because different cell types or tissues may express specific LRP1 co-receptors. In neurons and neurite-generating cell lines, indeed, N-methyl-D-aspartate receptor (NMDA-R) acts as an LRP1 co-receptor, physically linked to LRP1 by postsynaptic density protein 95, activating signaling factors, such as extracellular signal-regulated kinase 1/2 (ERK1/2) (Mantuano *et al.,* 2013). Trk receptors as well as NMDA-R have been also described as LRP1 co-receptors, essential for activation of Src, ERK1/2 and Akt in response to activated α2-macroglobulin and tPA (Shi *et al.,* 2009). Tissue plasminogen activator is a 527 aminoacid residue protein that contains two kringle domains and a proteolytic domain (Xanthopoulos *et al.,* 2005). tPA activates plasmin formation by cleaving plasminogen (Hoylaerts *et al.,* 1982; Kornblatt *et al.,* 2003). Moreover, it was previously suggested that the PrP^C interacts with kringle-bearing proteins (Ryou *et al.,* 2003) and Ellis et al. demonstrated that the PrP^C participates in the tPA-mediated plasminogen activation (Ellis *et al.,* 2002). In particular, they found that this complex, cleaves plasminogen to plasmin and the cleavage reaction was greatly accelerated (200 folds) by the presence of PrP^C (Praus *et al.,* 2003). The stimulatory activity is conserved in the NH_2-terminal fragment and the carboxy-terminal fragment that remains attached to the cell membrane via its GPI-anchor (Epple *et al.,* 2004).

Various mechanisms have been proposed to explain the activity of tPA in the CNS, including pathways that require binding to LRP1 and activation of LRP1-dependent cell signaling (Zhuo *et al.,* 2000; Samson *et al.,* 2008; Echeverry *et al.,* 2010), which in turn activates kinases such as ERK/MAPK (ERK1/2), promoting neuronal survival, and supporting neurite outgrowth (Holtzman *et al.,* 1995; Qiu *et al.,* 2004; Hayashi *et al.,* 2007; Fuentealba *et al.,* 2009).

In this study, we describe the role of lipid rafts in the recruitment and activation of downstream signal transduction pathways mediated by the interaction among tPA, PrP^C, and LRP1 in human neuroblastoma SK-N-BE2 cells. In our cell model, knocking-down PrP^C by siRNA impairs ERK phosphorylation induced by tPA and the alteration of the lipidic milieu of lipid rafts, perturbing the physical/functional interaction between PrP^C and LRP1, inhibits this response. We show that all these molecules are part of a single multimolecular signaling complex, whose activity depends strictly on the integrity of the lipid raft.

Materials and methods

Cell cultures and treatments

Human Neuroblastoma SK-N-BE2 cell line (ATCC Cat# CRL-2271, RRID:CVCL_0528) (not listed as misidentified cell line by ICLAC; authenticated 12/31/2014 and Frozen 10/21/2015; lot number 63600151), were maintained in Dulbecco's Modified Eagle Medium (DMEM cod. D6429, 2019) (Sigma-Aldrich, Milan, Italy), containing 10% fetal bovine serum (Euroclone, Milan, Italy - cod. ECS 0180L, 2018) plus 100 units/ml penicillin, 10 mg/mL streptomycin (Euroclone - cod. ECB3001D, 2018), at 37°C in humified CO_2 atmosphere and used within and not further than 5th passage. SK-N-BE2 cells were cultured until 80% confluent and then, where indicated, treated with 10 nM tPA (Molecular Innovations, Novi, MI, USA cod. HTPA-ALANC, 2018) for 10 min at 37°C.

To analyze the effect of disruption of lipid rafts, where indicated, cells were treated with 30 μM fumonisin B1 (FB1) (Sigma-Aldrich - cod. 34139, 2018), (a competitive inhibitor of ceramide synthetase) for 24 h at 37°C (Marasas *et al.,* 2004) or treated with 5mM methyl-β-cyclodextrin (MβCD) (Sigma-Aldrich - cod. 332615, 2018), a compound which is known to induce cholesterol efflux from the membrane for 30 min at 37°C (Whitehead *et al.,* 2012). After treatment, cells were collected and prepared for experimental procedures. Institutional ethical approval was not required for the study.

Sucrose-gradient fractionation and immunoblotting analysis

Lipid raft fractions were isolated as previously described (Mattei *et al.,* 2011). Briefly, 7×10^7 SK-N-BE2 cells, untreated and treated with 10 nM tPA (Molecular Innovations) for 10 min at 37°C, were suspended in 1 mL of lysis buffer, containing 1% Triton X-100 (Sigma-Aldrich - cod. 1610407, 2018), 10 mM Tris-HCl (pH 7.5), 150 mM NaCl, 5 mM EDTA, 1 mM Na_3VO_4 and 75 U of aprotinin and allowed to stand for 20 min. Cells were mechanically disrupted by Dounce homogenization (10 strokes). The lysate was centrifuged for 5 min at 1300 g to remove nuclei and large cellular debris. The supernatant (postnuclear fraction) was subjected to sucrose density gradient centrifugation: the supernatant lysate was mixed with an equal volume of 85% sucrose (w/v) in lysis buffer (10 mM Tris-HCl pH 7.5, 150 mM NaCl, 5 mM EDTA). The diluted lysate was placed at the bottom of a linear sucrose gradient (5–30%, in the same buffer) and centrifuged at 200.000 *g* for 18 h at 4°C using a SW41 rotor (Beckman Institute, Palo Alto, CA, USA). After centrifugation, the gradient was fractionated and 11 fractions were collected by volume starting from the top of the tube. All steps were carried out at 0–4°C. The fraction samples were loaded by volume and subjected to sodium dodecyl sulfate-polyacrylamide gel electrophoresis (SDS-PAGE) (10%). The proteins were electrophoretically transferred onto polyvinylidene difluoride (PVDF) membranes (Bio-Rad, Milan, Italy- cod. 1620177, 2018), blocked with 5% bovine serum albumin (BSA) in TBS containing 0.05% Tween 20 (TBS/T) and washed with TBS/T. Membranes were probed with anti-LRP1 (C-terminal) pAb (1 : 1000) (Sigma-Aldrich RRID:AB_10606463) or with anti-PrP SAF32 mAb (1 : 1000) (Spi-Bio, Bertin Pharma, France - cod. A03202, 2018) or with anti-CD71 mAb (1:1000) (Abcam, Cambridge, MA, USA - RRID:AB_10859929) or with anti-Flotillin pAb (1 : 1000) (Santacruz Biotechnologies, Heidelberg, Germany - cod. sc-48398, 2018). After washing with TBS/T, bound antibodies were visualized with HRP-conjugated anti-rabbit IgG (1 : 5000) (Cell Signaling Technology Danvers, MA, USA - RRID:AB_2099233) or HRP-conjugated anti-mouse IgG (1 : 5000) (Cell Signaling Technology - RRID:AB_330924) and immunoreactivity was assessed by chemiluminescence reaction, using the ECL Western detection system (TermoFisher Scientific, MA, USA - cod. 32106, 2018). Densitometric scanning analysis was performed by Mac OS X (Apple Computer International), using NIH Image 1.62 software. The density of each band in the same gel was analyzed, values were totaled, and then the percent distribution across the gel was detected.

Immunoprecipitation experiments

SK-N-BE2 cells, untreated or treated with 10 nM tPA (Molecular Innovations) for 10 min at 37°C, were lysed in lysis buffer (10 mM Tris-HCL pH 8.0, 150 mM NaCl, 1% Nonidet P-40, 1 mM phenylmethylsulfonyl fluoride, 10 mg/mL leupeptin). Cell-free lysates were mixed with protein G-acrylic beads (Sigma-Aldrich, - cod. P3296, 2018) and stirred by a rotary shaker for 2 h at 4°C to pre-clear nonspecific binding. After centrifugation (500 *g* for 1 min), the supernatant was immunoprecipitated with rabbit anti-LRP1 pAb (2 μg) (Sigma-Aldrich), plus protein G-acrylic beads. After vigorous mixing for 5 min, samples were further mixed. As a negative control, immunoprecipitation was performed with an irrelevant rabbit IgG (2 μg) (Sigma-Aldrich - RRID:AB_1163659). The immunoprecipitates were split into two aliquots. The first one was subjected to Western blot analysis for PrP^C, or LRP1 detection; the second one was checked by dot blot for GM1 detection.

Immunoblotting analysis of immunoprecipitates

The immunoprecipitates, obtained as reported above, were subjected to SDS-PAGE. The proteins were electrophoretically transferred onto PVDF membranes. Membranes were blocked with 5% bovine serum albumin (BSA) in TBS/T and subsequently washed with TBS/T. The membranes were probed with: anti-PrP^C SAF32 mAb (Spi-Bio) or anti-LRP1 mAb (Abcam). After washing with TBS/T, bound antibodies were visualized with HRP-conjugated anti-mouse IgG (1 : 5000) and immunoreactivity assessed by chemiluminescence reaction, using the ECL western detection system.

Dot-Blot analysis of immunoprecipitates

Briefly, aliquots of LRP1 immunoprecipitates, prepared as described above, were spotted onto nitrocellulose strips. The strips were blocked for 1 h with 5% BSA in TBS/T (Bio-Rad - cod. 170-6435, 2019), (Bio-Rad - cod. 170-6531, 2018), to block the residual binding sites on the paper. The strips were rinsed for 10 min in TBS/T and then incubated with Cholera Toxin B Subunit-Peroxidase from Vibrio Cholerae (1 : 2000) (Sigma-Aldrich- cod. C1655, 2018) for 1 h at 25°C, or with anti-LRP1 mAb (1 : 1000) (Abcam - RRID:AB_881181) and further incubated for 1 h at 37°C with HRP-conjugated anti-mouse IgG (1 : 5000) (Cell Signaling Technology). Immunoreactivity was assessed by chemiluminescence reaction, using the ECL Western detection system.

Knockdown PrP^C and LRP1 by siRNA

SK-N-BE2 cells were seeded (2×10^5 cells/mL) 6-well plate, in DMEM containing serum and antibiotics. Twenty-four hours after

seeding, cells were transfected with 5 nM siRNA PrP (Qiagen, Valencia, CA, USA - cod. GS5621, 2018) or 5 nM siRNA LRP1 (Qiagen - cod. GS4035, 2018) (Table 1), using HiPerFect Transfection Reagent (Qiagen - cod. 1027281, 2018), according to the manufacturer's instructions. As experimental control, cells were also transfected with 5-nM scrambled siRNA (AllStars Negative Control - Qiagen). After 72 h, the expression of PrP^C and LRP1 was evaluated by immunoblotting analysis using anti-PrP^C SAF32 mAb or anti-LRP1 pAb (Sigma-Aldrich). Parallel cell samples were incubated with 10 nM tPA (Molecular Innovations) for 10 min at 37°C or alternatively for 10 days in the same conditions. For long-time exposure with tPA (10 days) every 4 days siRNA PrP and siRNA LRP1 were replaced.

tPA activity assay

The human chromogen activity analysis commercial kit for the plasminogen activator was used, according to the manufacturer's instructions (Abcam - cod. ab108905, 2018). The test measures the ability of the tPA to activate plasminogen in plasmin in dosage systems containing tPA, plasminogen and a specific synthetic substrate of plasmin. The amount of plasmin produced is quantified using a highly specific plasmin substrate, which releases a yellow paranitroaniline chromophore (pNA). The change in pNA absorbance in the 405 nm reaction solution is directly proportional to the activity of the tPA enzyme. We analyzed supernatants from cell cultures not treated or treated with tPA 10 nM (Prospec, Ness Ziona, Israel - cod. enz-263, 2018), in the presence or absence of pretreatment with siRNA PrP or siRNA LRP1 and/or 5 mM MβCD, as described above. The evaluation of tPA activity in the supernatants of the various samples prepared allows us to indirectly assess the functionality of the cellular tPA receptor system. In fact, when the tPA receptor system is altered, the tPA molecules will not be able to interact with the cells, thus remaining in the culture supernatant in which we measure their activity. The amount of active tPA still present in the supernatant expresses the amount of tPA that was not able to bind to the cellular receptor system.

ERK pathway activation analysis

The activation of ERK pathway and the role of lipid raft was assessed by Western blot in SK-N-BE2 cells, untreated or treated with 10 nM tPA in the presence of 5 mM MβCD (Sigma-Aldrich) for 30 min at 37°C or FB1 (Sigma-Aldrich) for 24 h at 37°C. Briefly, SK-N-BE2 sample was lysed in lysis buffer containing 0.1% Triton X-100, 10 mM Tris-HCl (pH 7.5), 150 mM NaCl, 5 mM EDTA, 1 mM Na3VO4 and 75 U of aprotinin and allowed to stand for 20 min at 4°C. The cell suspension was mechanically disrupted by Dounce homogenization (10 strokes). Each lysate, numbered and coded, was centrifuged for 5 min at 1300 *g* to eliminate nuclei and large cellular debris and, after protein concentration analysis by Bradford Dye Reagent assay (Bio-Rady-cod. 5000006, 2018), the lysate was tested with SDS-PAGE. Subsequently, the proteins were electrophoretically transferred to PVDF membranes (Bio-Rad), then blocked with 5% BSA in TBS (Bio-Rad), containing 0.05% Tween 20 (Bio-Rad), and probed with anti-phospho ERK1/2 (p-ERK1/2) (Thr202/tyr204) pAb (1 : 1000) (Cell Signaling Technology - RRID:AB_331646) or anti-total ERK1/2 (t-ERK1/2) pAb (1 : 1000) (Cell Signaling Technology - RRID:AB_330744). Antibodies were visualized with horseradish peroxidase (HRP)-conjugated anti-rabbit IgG (GE Healthcare Amersham Biosciences, Uppsala, Sweden) and immunoreactivity assessed by chemiluminescence reaction, using the ECL detection system (Amersham, Buckingamshire, UK). Densitometric scanning analysis was accomplished with NIH Image 1.62 software by Mac OS X (Apple Computer International) and scored by two investigators blinded to treatment groups.

Immunofluorescence analysis

SK-N-BE2 cells were seeded (2×10^5 cells/mL) in 6-well plate in DMEM containing serum and antibiotics. Twenty-four hours after seeding, cells were treated with siRNA PrP (Qiagen) or MβCD as described extensively above and then stimulated with 10 nM tPA for 10 days. Every four days, siRNA PrP was replaced. After 10 days, the cells were used for immunofluorescence analysis. Briefly, SK-N-BE2 treated as above was fixed with 4% paraformaldehyde (Euroclone - cod. APA38131000, 2018) and permeabilized by 0.1% (v/v) Triton X-100. After washing, cells were incubated with rabbit anti-GAP43 mAb (1 : 200) (Cell Signaling Technology - RRID:AB_10860076) for 1 h at 4°C, followed by anti-rabbit Alexa fluor 488 (1 : 50) (Cell Signaling Technology - RRID:AB_1904025) for additional 30 min. Each well containing a stained cell sample was numbered and coded. Sprouting frequencies were scored by two investigators blinded to treatment groups. Differences in sprouting frequency were tested by ANOVA. Treatment means were analyzed by a Multiple comparisons test. Finally, cells were observed with a Zeiss Axio Vert. A1 fluorescence microscope (Zeiss, Milan, Italy).

Statistical analysis

All the statistical procedures were performed by GraphPad Prism Software Inc. (San Diego, CA, USA). Data were analyzed using one-way analysis of variance (ANOVA, XLSTAT 2019.2) after Bartlett's test for the homogeneity of variances and Kolmogorov–Smirnov's test for the Gaussian distribution and followed by Newman–Keuls multiple-comparison test or, when appropriate, with Student's t-test. All data reported were verified in at least three different experiments and showed as scatter plots. The horizontal bars indicate the mean. For the outliers, Grubb's method was used, no data points were excluded. Only p values of < 0.05 were considered as statistically significant.

Results

Distribution of PrP^C and LRP1 in sucrose density gradient fractions

PrP^C, like many GPI-anchored proteins, resides within Triton X-100-insoluble, cholesterol, and sphingolipid-rich rafts in neuronal cells. Although PrP^C is already known to be enriched in lipid microdomains, we first analyzed the distribution of this molecule in both Triton X-100-insoluble and -soluble fractions of cell plasma membranes before and after tPA triggering. Next, the same analysis was carried out for LRP1 too. As shown in Fig. 1a, the analysis of PrP^C distribution in fractions obtained with a 5–30% linear sucrose gradient confirmed that in control cells the majority of PrP^C was distributed in fractions 4–6, corresponding to lipid raft.

This predominant distribution was more evident in tPA stimulated cells. These results were quantified by densitometric analysis (right panel).

As expected, the majority of LRP1 was distributed in the Triton X 100-soluble fractions 9-11 obtained from control cells, while after treatment with tPA, the majority of this protein was redistributed to the Triton X 100-insoluble fractions 4-6 (Fig. 1b), as confirmed by densitometric analysis (right panel).

As controls, the distribution of the transmembrane transferrin receptor (CD71), as Triton X-100 soluble protein and of Flotillin as a marker of lipid raft, was tested in the same sucrose density gradient fraction separation experiment. CD71 appeared to be clearly distributed mainly in the Triton X-100-soluble fractions (9-11) in both control and tPA-treated cells (Fig. 1c). In contrast, the majority of Flotillin appeared in Triton X-100-insoluble fractions (4-6) in both control and tPA-treated cells (Fig. 1d). These results were also quantified by densitometric analyses.

LRP1 is recruited to lipid rafts and associates with PrP^C following tPA stimulation

In order to evaluate: a) the interaction of PrP^C with LRP1, and b) the influence of tPA on the association of the two molecules, co-immunoprecipitation experiments were performed. A rabbit anti-LRP1 pAb was used to immunoprecipitate LRP1 on a SK-N-BE2 neuroblastoma cell line, untreated or treated with tPA, which is known as a LRP1 ligand, able to initiate cellular signaling in neuron-like cells. Western blot analysis, using anti-PrP SAF32 mAb, was employed to evaluate the LRP1-PrP^C interaction. It showed a band of co-immunoprecipitation reacting with the anti-PrP mAb, which was more evident in cells stimulated with tPA, indicating an increased interaction of the two molecules, LRP1 and PrP^C, after tPA treatment (Fig. 2a, and densitometric analysis, right panel). In both untreated and tPA treated samples, no bands were detected in control immunoprecipitation experiments carried on using an IgG having irrelevant specificity. LRP1 immunoprecipitate was checked by an anti-LRP1 mAb.

Moreover, to investigate the recruitment of LRP1 to lipid rafts following tPA stimulation, we studied the possible interaction of LRP1 with the ganglioside GM1, a well-known raft marker. Dot blot analysis performed on LRP1-immunoprecipitated samples revealed that in unstimulated control cells, GM1 was weakly associated with LRP1, but, after tPA treatment, the association of GM1 with LRP1 significantly increased (Fig. 2b, and densitometric analysis (right panel). Virtually no spots were detected in control immunoprecipitation experiments carried on using an IgG having irrelevant specificity. LRP1 immunoprecipitate was checked by an anti-LRP1 mAb.

tPA works through its association with PrP^C and LRP1 in a multimolecular signaling complex, strictly dependent from lipid raft

As already reported (Ellis *et al.* 2002; Kornblatt *et al.* 2003; Ryou *et al.,* 2003), tPA catalyzes the activation of plasminogen by binding the fibrin or other molecules of the cell surface and this activity has been suggested to be regulated by PrP^C, which then acts as a cofactor. We analyzed in SK-N-BE2 cells: a) whether tPA activity in its function of plasminogen activator is, in our cell system, actually dependent on PrP^C, b) whether the demonstrated association of PrP^C with LRP1 plays a role in the tPA activity, c) the involvement of lipid rafts.

For this aims, we used a tPA activity determination kit to analyze the supernatants of cell cultures stimulated with tPA. The rationale of this experiment is based on the fact that the tPA administered to a cellular system acts by binding to the deputy receptor system. If this receptor system is altered, the tPA molecules will be unable to interact with the cells remaining in the supernatant of the culture. Therefore, the evaluation of tPA activity in the supernatants of the various samples prepared, allows us to indirectly evaluate the functionality of the receptor system of the cell.

In order to evaluate the involvement of PrP^C and/or LRP1 in the tPA function, SK-N-BE2 cell culture were treated with a small interfering RNA (siRNA PrP or siRNA LRP1). Under our experimental conditions, we found that 72 h after siRNA PrP treatment, SK-N-BE2 cell culture showed a significant reduction of PrP^C (about 80%), as compared to scrambled siRNA-transfected cells (Fig. 3a). In cells transfected with siRNA LRP1 a significant reduction (about 60%)

Fig. 1 Lipid microdomain localization of low-density lipoprotein receptor-related protein 1 (LRP1) and PrP^C in SK-N-BE2 cells. Representative immunoblots of sucrose gradient fractions. SK-N-BE2 cells, either untreated or treated with 10 nM tPA for 10 min at 37°C, were lysed and the supernatant fraction was subjected to sucrose density gradient. After centrifugation, the gradient was fractionated and each fraction was recovered and analyzed by western blot using the following: (a) an anti-PrP SAF32 mAb; (b) and anti-LRP1 pAb. Right panel Densitometric analysis of sucrose gradient fractions. Scatter plot indicates the percent distribution across the gel of raft-fractions 4–5 and 6 (Triton X-100-insoluble fractions) and 9–10 and 11 (Triton X-100-soluble fractions), as detected by densitometric scanning analysis. The horizontal bars indicate the mean. The data are presented as densitometric units from three independent cell culture preparations (*)$p < 0.01$ TX-100-insoluble fractions from tPA-treated cells versus TX-100-insoluble from control cells; (°) $p < 0.01$ TX-100-soluble fractions from tPA-treated cells versus TX-100-soluble from control cells. As controls, fractions obtained after sucrose density gradient from untreated or treated cells were analyzed using an anti-CD71 mAb (c) or an anti-flotillin pAb (d).

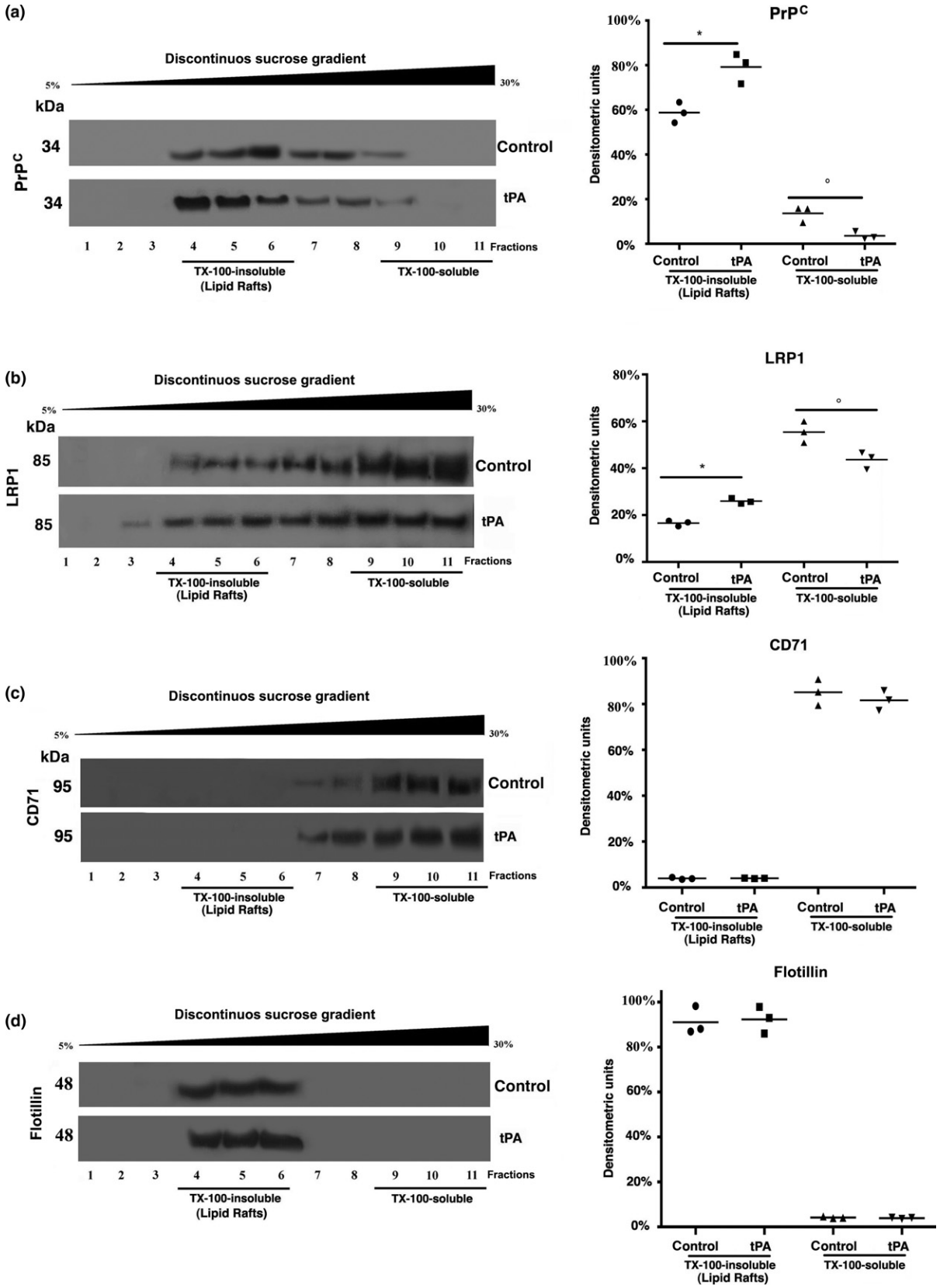
(a)
Discontinuos sucrose gradient
5%
30%
kDa
34
PrPC
Control
34
tPA
1 2 3 4 5 6 7 8 9 10 11 Fractions
TX-100-insoluble (Lipid Rafts)
TX-100-soluble
PrPC
Densitometric units
100%
80%
60%
40%
20%
0%
Control tPA Control tPA
TX-100-insoluble (Lipid Rafts)
TX-100-soluble
(b)
Discontinuos sucrose gradient
5%
30%
kDa
85
LRP1
Control
85
tPA
1 2 3 4 5 6 7 8 9 10 11 Fractions
TX-100-insoluble (Lipid Rafts)
TX-100-soluble
LRP1
Densitometric units
80%
60%
40%
20%
0%
Control tPA Control tPA
TX-100-insoluble (Lipid Rafts)
TX-100-soluble
(c)
Discontinuos sucrose gradient
5%
30%
kDa
95
CD71
Control
95
tPA
1 2 3 4 5 6 7 8 9 10 11 Fractions
TX-100-insoluble (Lipid Rafts)
TX-100-soluble
CD71
Densitometric units
100%
80%
60%
40%
20%
0%
Control tPA Control tPA
TX-100-insoluble (Lipid Rafts)
TX-100-soluble
(d)
Discontinuos sucrose gradient
5%
30%
48
Flotillin
Control
48
tPA
1 2 3 4 5 6 7 8 9 10 11 Fractions
TX-100-insoluble (Lipid Rafts)
TX-100-soluble
Flotillin
Densitometric units
100%
80%
60%
40%
20%
0%
Control tPA Control tPA
TX-100-insoluble (Lipid Rafts)
TX-100-soluble

of LRP1 was detectable, with respect to scrambled siRNA-transfected cells (Fig. 3a).

Furthermore, in order to evaluate the role of lipid rafts, we analyzed tPA activity in the same samples from cell cultures in the presence of MβCD, a compound able to induce cholesterol efflux from the membrane (Whitehead *et al.,* 2012), which is known to disrupt the lipid raft structure, preventing its functions.

The results reported in Fig. 3b showed that a significantly higher residual activity of tPA was present in the supernatants of MβCD + tPA-treated cells as compared to cells treated with tPA only. Interestingly, the supernatants of cells treated with PrP siRNA, as well as with LRP1 siRNA also revealed a significantly higher residual activity of tPA as compared to control cells (scrambled + tPA). This effect in siRNA cells was exacerbated in the presence of MβCD treatment.

The reported data showed that the residual tPA activity in supernatants is significantly detectable only in those samples in which the putative multimolecular receptor complex has been disabled. Thus, these results clearly indicated that PrP, LRP1 and lipid raft integrity are essential for tPA binding and function.

Knocking-down PrP^C and LRP1 by siRNA impairs signal transduction induced by tPA

Cells treated with siRNA PrP were stimulated with tPA for 10 min at 37°C and analysed by Western blot using an anti-phospho-ERK1/2 pAb. The result revealed that the phosphorylation of ERK1/2 was significantly reduced, as compared to siRNA PrP transfected cells (Fig. 4a).

In parallel experiments, LRP1 siRNA-treated cells were incubated with tPA and analysed by Western blot using an anti phospho-ERK1/2 Ab. It revealed that

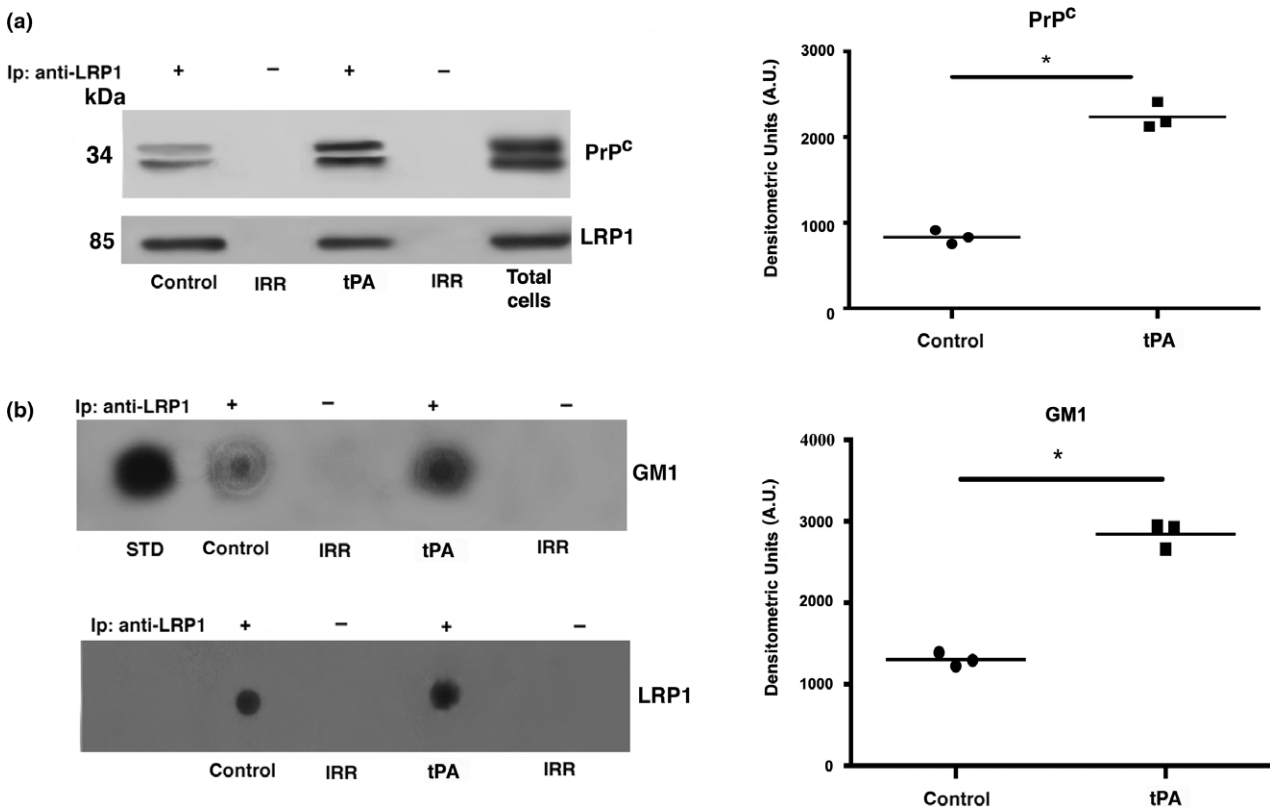

Fig. 2 Low-density lipoprotein receptor-related protein 1 (LRP1) associates with PrP^C and ganglioside GM1 under tPA stimulation. SK-N-BE2 cells, untreated or treated with 10 nM tPA, were lysed in lysis buffer, followed by immunoprecipitation with rabbit anti-LRP1 pAb. A rabbit IgG isotypic control (IRR) was employed. (a) The immunoprecipitates were analyzed for the presence of PrP^C by Western blot analysis, using anti-PrP SAF32 mAb. A representative experiment among three is shown. As a control, the immunoprecipitates were assessed by immunoblot with anti-LRP1 mAb. Scatter plot shows densitometric analysis from three independent cell culture preparations. The horizontal bars indicate the mean. (*) $p < 0.01$ tPA versus control cells. (b) Standard GM1 (STD) and the immunoprecipitates were spotted onto nitrocellulose strips and incubated with Cholera Toxin B Subunit-Peroxidase (from Vibrio Cholerae) as described in Materials and Methods. As a control, the immunoprecipitates were assessed by Dot-blot with anti-LRP1 mAb. A rabbit IgG isotypic control (IRR) was employed. A representative experiment among three is shown. Scatter plot shows densitometric analysis. The horizontal bars indicate the mean. The data are presented as densitometric units from three independent cell culture preparations. (*)$p < 0.01$ tPA versus control cells.

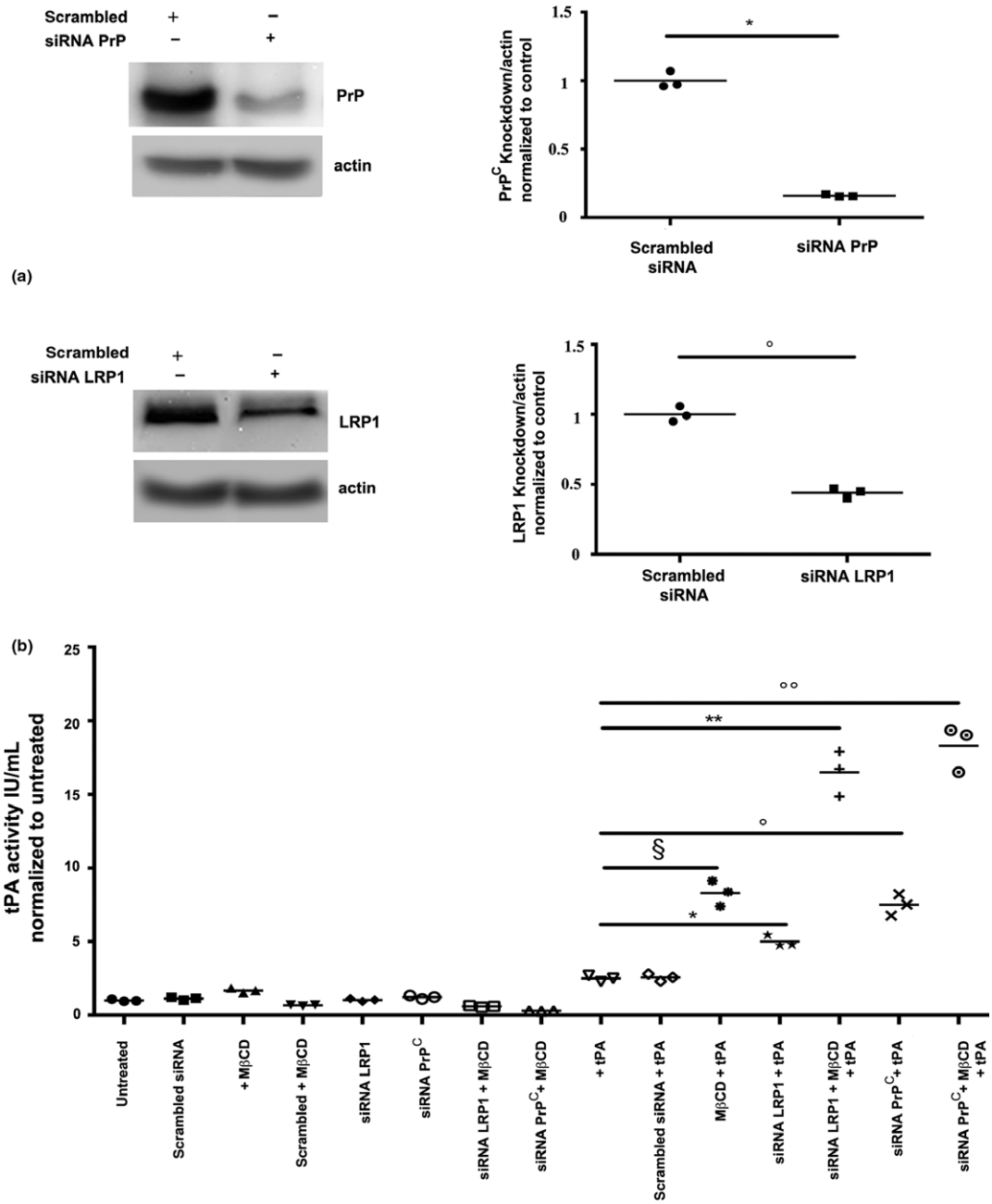

Fig. 3 tPA activity levels in the SK-N-BE2 supernatants. (a) Evaluation of PrP^C and low-density lipoprotein receptor related protein 1 (LRP1) expression after 72 h siRNA transfection by Western blot analysis using anti-PrP SAF 32 mAb and anti-LRP1 pAb. A scrambled siRNA was used as control. Scatter plot in the right panel shows densitometric analysis. The horizontal bars indicate the mean. The data are presented as densitometric units from three blinded independent cell culture preparations. (*)$p < 0.01$ siRNA PrP versus scrambled siRNA and (°)$p < 0.01$ siRNA LRP1 versus scrambled siRNA. (b) Analysis of Tissue type Plasminogen Activator Human Chromogenic Activity Assay in SK-N-BE2 supernatants, untreated or treated with 10 nM tPA, in the presence or in the absence of pre-treatment with siRNA PrP or siRNA LRP1, or in the association or in the absence with 5 mM methyl-β-cyclodextrin (MβCD). Scatter plot shows densitometric analysis. The horizontal bars indicate the mean. The data are presented as densitometric units from three independent experiments. (§)$p < 0.01$ MβCD + tPA versus tPA-treated cells; (*)$p < 0.01$ siRNA LRP1 + tPA versus tPA-treated cells, (**)$p < 0.01$ siRNA LRP1 + MβCD + tPA versus tPA-treated cells, (°)$p < 0.01$ siRNA PrP + tPA versus tPA-treated cells, (°°)$p < 0.01$ siRNA + MβCD + tPA versus tPA-treated cells.

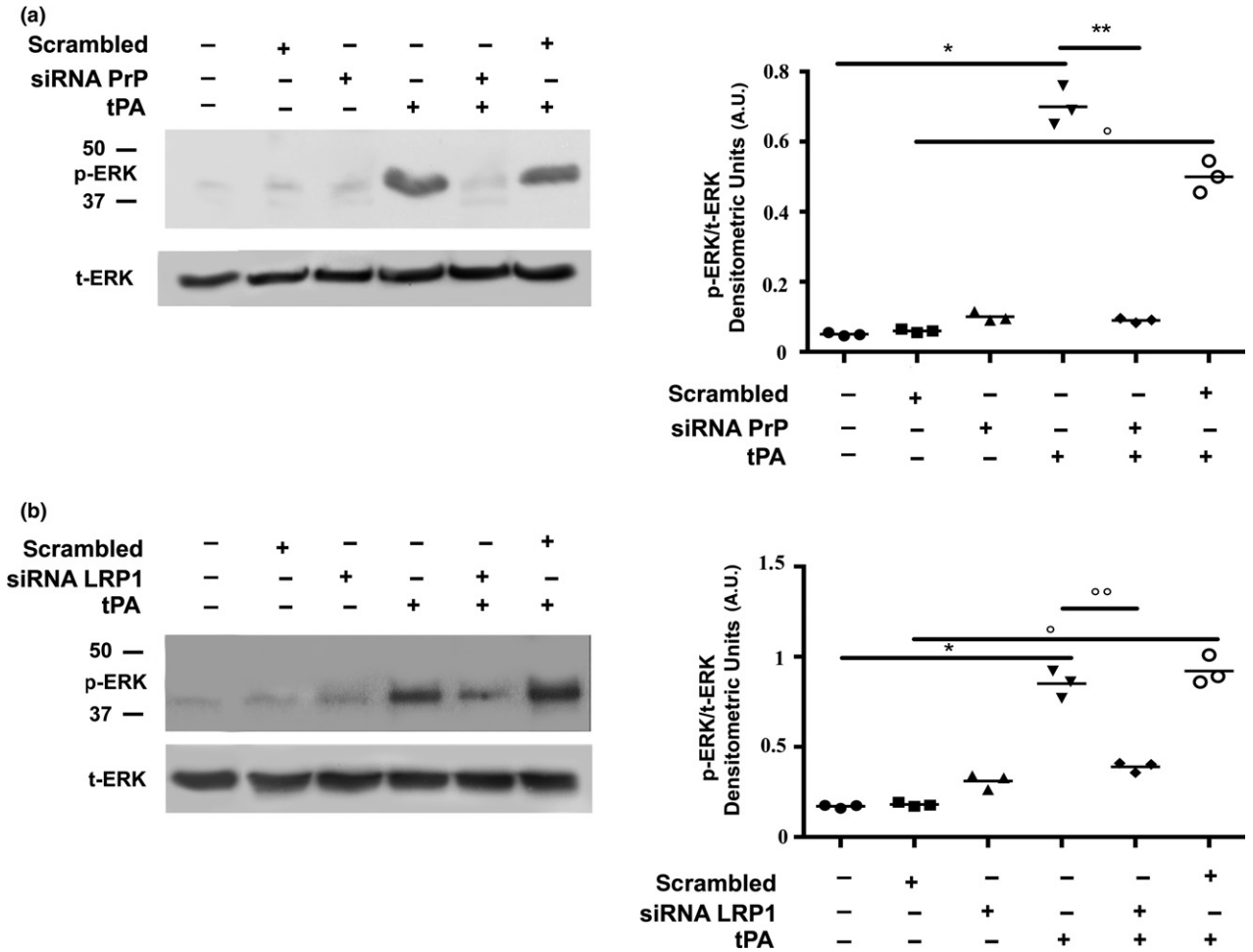

Fig. 4 Effect of PrP^C or low-density lipoprotein receptor-related protein 1 (LRP1) silencing on ERK phosphorylation induced by tPA in SK-N-BE2 cells. SK-N-BE2 cells, untreated or treated with 10nM tPA, in the presence or in the absence of pre-treatment with siRNA PrP (a) or siRNA LRP1 (b) were analyzed by Western blot, using anti-phospho ERK1/2(p-ERK1/2) (Thr202/tyr204) pAb or anti-total ERK1/2(t-ERK1/2) pAb (Cell Signaling Technology). Scatter plot shows densitometric analysis. The horizontal bars indicate the mean. The data are presented as densitometric units from 3 independent blinded experiments. (*)$p < 0.01$ tPA-treated cells versus untreated cells, (°) $p < 0.01$ scrambled siRNA + tPA-treated cells versus scrambled siRNA, **$p < 0.01$ siRNA PrP + tPA-treated cells versus tPA-treated cells, °°$p < 0.01$ siRNA LRP1 + tPA-treated cells versus tPA-treated cells.

the phosphorylation of ERK1/2 was significantly reduced, as compared to siRNA LRP1 transfected cells (Fig. 4b).

Effect of Lipid rafts disruption on tPA function through the multimolecular complex

Gangliosides and cholesterol are structural components of lipid rafts. Two different agents capable to perturb lipid rafts integrity have been considered: MβCD and FB1, a ceramide synthase inhibitor (Marasas *et al.,* 2004). Both effectors have the capability to disrupt lipid raft structure and function (Fig. S1).

By the use of these molecules, we investigated whether the integrity of the lipid microdomains may play a role in signaling induced by tPA.

SK-N-BE2 cells were pre-incubated with FB1 or with MβCD and then stimulated with tPA for 10 min at 37°C. As shown in Fig. 5, Western blot analysis using a specific anti-phospho-ERK1/2 (p-ERK1/2), indicated that tPA treatment significantly enhanced phosphorylation of ERK1/2, which was counteracted by pre-treatment with FB1 or MβCD. These results were also confirmed by densitometric analysis (Fig. 5, right panel bar graphs). Thus, these findings suggest a role for lipid rafts in the signal transduction pathway triggered by tPA.

Prion protein and MβCD affected neurite outgrowth induced by tPA in SK-N-BE2

It has been reported that tPA is able to induce neurite outgrowth in neuronal progenitor cells (Lee *et al.,* 2014). The

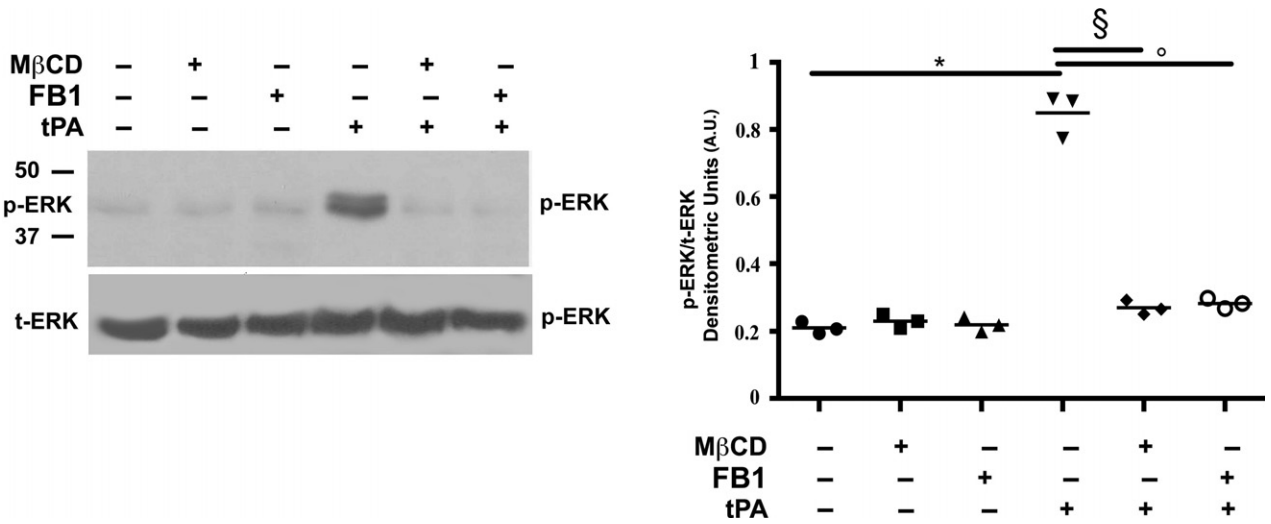

Fig. 5 Effect of raft disruption on ERK phosphorylation induced by tPA in SK-N-BE2 cells. SK-N-BE2 cells, untreated or treated with 10 nM tPA, in the presence or in the absence of pre-treatment with 5 mM methyl-β-cyclodextrin (MβCD) or FB1 were analyzed by Western blot, using anti-phospho ERK1/2(p-ERK1/2) (Thr202/tyr204) pAb or anti-total ERK1/2(t-ERK1/2) pAb (Cell Signaling Technology). Scatter plot shows densitometric analysis. The horizontal bars indicate the mean. The data are presented as densitometric units from three independent blinded experiments. (*)$p < 0.01$ tPA-treated cells versus untreated cells; (§)$p < 0.01$ MβCD + tPA-treated cells versus tPA-treated cells (°)$p < 0.01$ FB1 + tPA-treated cells versus tPA-treated cells.

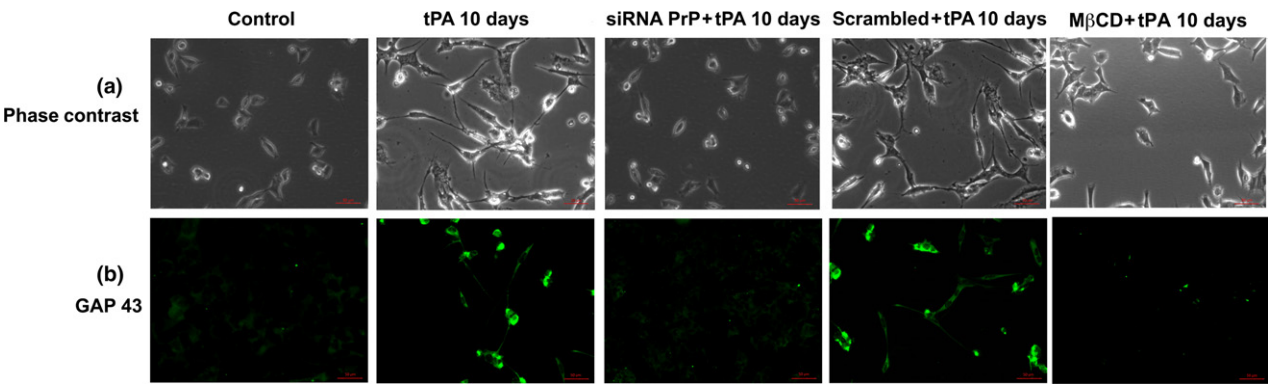

Fig. 6 Knocking-down PrP^C gene and methyl-β-cyclodextrin (MβCD) affected neurite outgrowth induced by tPA. SK-N-BE2 cells untreated and treated with siRNA PrP, MβCD or scrambled siRNA for 72 h were stimulated with tPA for 10 days and analyzed by immunofluorescence analysis. Scale bars, 100 μm. (a) Morphology of SK-N-BE2 cell lines; (b) Immunofluorescence analysis of neuronal marker GAP43. A representative experiment among three blinded experiments is shown.

neurite outgrowth regulation by tPA plays a role in plasminogen activation and is involved in pathological conditions or regeneration (Pittman *et al.,* 1989).

In order to study the involvement of PrP^C and MβCD molecules in the neurite outgrowth induced by tPA, we cultured SK-N-BE2 cells in the presence or in the absence of tPA (10 days). Phase contrast microscopy showed, as expected, an evident morphological differentiation of cells incubated with tPA compared to control. When the cells were pre-treated with siRNA PrP or MβCD, the tPA-mediated neurite outgrowth was affected (Fig. 6a). Morphological data were quantified and confirmed by using NeuronJ plugin from the ImageJ package Fiji, a commonly used tool for semiautomatic tracing and measurement of neurites in ImageJ (Schindelin *et al.,* 2012; Pemberton *et al.* 2018) (Fig. S2). For each treatment group, actual measurements of neurite length and branch number were performed by two observers in a double-blind manner, as described in Material and Methods section.

Immunofluorescence staining using a mAb anti GAP-43, as neuronal differentiation marker, further confirmed the morphological result. In Fig. 6b, it is reported an anti-GAP43 staining indicating the role of PrP^C and MβCD in the neurite outgrowth by tPA. Again, cells treated with tPA in the

Table 1 siRNA PrP and siRNA LRP1 sequences

Flexitube GeneSolution GS5621 for PRNP	GeneGlobe Catalog number	Flexitube GeneSolution GS4035 for LRP1	GeneGlobe Catalog number
TAGAGATTTCATAGCTATTTA	SI03019625	TACGACCGCATCGAGACGATA	SI03109400
CAGCAAATAACCATTGGTTAA	SI03019324	CTGGCTATTGACTTCCCTGAA	SI00036204
CTGAATCGTTTCATGTAAGAA	SI04351298	CCGGAGTGGTATTCTGGTATA	SI00036197
CAGTGACTATGAGGACCGTTA	SI04244828	CCGCCGGATGTATAAATGTAA	SI00036190

presence of siRNA PrP or MβCD, showed an evident decrement of the GAP43 staining compared to tPA-treated cells, indicating an under regulation of tPA differentiative effect. GAP43 immunofluorescence was quantified for fluorescence intensity using ImageJ (Fig. S3). For each treatment group, actual measurements of neurite length and branch number were performed by two observers in a double-blind manner.

Discussion

In this paper, we demonstrate that tPA, PrP^C, and LRP1 are all together molecules forming a unique multimolecular signaling complex, whose activity is strictly dependent on lipid raft.

It is well known that lipid rafts associate and quickly dissociate themselves forming functional clusters (Sonnino and Prinetti 2012) and these clusters favor the interaction of specific proteins with lipid molecules. Such molecular associations are highly efficient in membrane trafficking and cellular signaling (Simons, 2000; Barbat *et al.,* 2007), allowing the lateral segregation of proteins within the membranes, providing a mechanism for the partitioning and concentration of signaling components (Simons, 1997; Pizzo and Viola 2003; Garofalo *et al.,* 2003).

In neurons, lipid rafts have been implicated in the recruitment of proteins involved in neurotransmitter signaling. Rafts facilitate the transport and regulate the release of the neurotransmitters, recruit the receptor molecules to the synapse and the associated signal transduction molecules (Aureli *et al.,* 2015).

Mantuano et al. have shown that, when neuronal cells are treated with tPA, LRP1 forms a complex with other membrane molecules (Mantuano *et al.,* 2013) and this complex seems to be indispensable for intracellular signaling that leads to biological responses such as neurite growth (Tsui-Pierchala *et al.,* 2002; Mantuano *et al.,* 2013; Lee *et al.,* 2014).

In this environment, it is not surprising that a molecule that has been shown to interact with PrP and, at the same time, bind LRP1, may act as a recruiter of molecules that are induced to interact with lipid raft only in particular conditions.

In fact, LRP1 in lipid rafts belongs to that subpopulation of dynamic receptors which can be transiently recruited into lipid rafts, more often it is localized in clathrin-coated wells, where it is subjected to endocytosis (Wu and Gonias 2005). Once the endocytic process has been initiated, LRP1 enters an intracellular vesicle transport pathway, which allows it to recycle to the cell surface with almost 100% efficiency (Willingham *et al.,* 1980; Dickson *et al.,* 1981). Therefore, although LRP1 is well known as an endocytic receptor, it can also function as a cellular signaling molecule, in specific cell types (Gonias and Campana 2014). In this particular case, we show that LRP1 can transiently be localized within lipid rafts. In this position, LRP1 is concentrated and probably interacts with other proteins, such as PrP^C, or NMDA-R (Mantuano *et al.,* 2015).

On the other hand, Praus et al. (Praus *et al.,* 2003) demonstrated that tPA-mediated plasminogen activation is dependent on tPA interaction with PrP^C and hypothesized that the interactions among PrP^C, tPA and plasminogen may play a role in the regulation of cellular proteolysis and could constitute a biological function of PrP^C. It means that the specific stimulation of tPA-mediated plasminogen activation by PrP^C suggests a further biological function of PrP^C. In the absence of fibrin, it might serve as a cofactor in the regulation of plasminogen activation by tPA in the central nervous system.

PrP^C is, however, neuroprotective and plays important roles in defense against neuronal oxidative stress and in the homeostasis of metal ion in the brain (Taylor and Hooper, 2006). Recently, PrP^C was identified as a high-affinity receptor for Aβ oligomers (Chen *et al.,* 2010), and the presence of PrP^C in hippocampal slices was responsible for the Aβ oligomer-mediated inhibition of LTP (Laurén *et al.,* 2009). Moreover, PrP-mediated toxicity of Amyloid-β oligomers requires lipid rafts and LRP1 transmembrane (Rushworth *et al.,* 2013). Several ligands of this, both endocytic and cell-signaling receptor, control the activity of LRP1 by directing the recruited co-receptors. It has been demonstrated that LRP1 controls both the surface and biosynthetic trafficking of PrP^C in neurons (Parkyn *et al.,* 2008). As LRP1, other LRPs have been implicated in the raft-association, internalization, and amyloidogenic processing of amyloid precursor protein (APP) (Pietrzik *et al* 2002; Cam *et al* 2005; Yoon *et al.* 2005) and thus play a role in the pathogenesis of neurodegenerative diseases, by altering the catabolism of LRP's ligands (eg IGF-I, ApoE/ lipoprotein/

cholesterol, tPA and α2M) and/or influencing metabolism and accumulation of Aβ, such as LRP6 in Alzheimer's Disease (AD) and APP processing (De Ferrari *et al.* 2007). It is interesting to note that the cytoplasmic domain of LRP has been shown to facilitate the association between the APP and the β-site APP cleaving enzyme 1 (BACE1) and improves APP delivery in rafts lipid through the endocytic pathway (Yoon *et al* 2007; Vetrivel and Thinakaran 2010; Spuch *et al* 2012).

Our results demonstrated that LRP1 is recruited to lipid rafts and associates with PrP^C under tPA stimulation in SK-N-BE2 cells, where co-immunoprecipitation experiments clearly indicated the interaction between the two proteins. From a theorical point of view, we cannot exclude the possibility that a subfraction of LRP1 in the non-raft region might associate with a minor pool of PrP in the non-raft fraction following tPA treatment and this complex could be then translocated to rafts. Moreover, co-immunoprecipitation with LRP1 and ganglioside GM1 further supports the recruitment of LRP1 into the lipid raft. This peculiar behavior of the LRP1 has been already suggested in our previous work (Laudati *et al.,* 2016) and the new data confirm and extend this previous indication. Indeed, in this report we clearly demonstrated that knocking-down PrP^C and LRP1 by siRNA impairs signal transduction induced by tPA and that the raft disruption by MCD or FB1 has a robust blocking effect on the tPA function through the multimolecular complex.

We demonstrated in this paper that in SK-N-BE2 cells, the absence of PrP^C affected neurite outgrowth induced by tPA. Moreover, the neurite outgrowth regulation by tPA plays a role in plasminogen activation and is involved in pathological conditions or regeneration (Lee *et al.,* 2014).

The results of this study show that PrP^C is strictly associated with gangliosides in lipid rafts of neuroblastoma cells, indeed co-immunoprecipitation analysis reveals a consistent association between PrP^C and GM1, as well as between LRP1 and GM1, indicating the existence of a glycosphingolipid-enriched molecular complex. These data taken together, suggest that LRP1 and PrP^C, following tPA stimulation, may function as a part of a single system associated with lipid rafts, involved in receptor-mediated neuritogenic pathway. We hypothesize that the ability of PrP^C to induce cell signaling may involve a multi-receptor complex, in which LRP1, in association with other receptors like NMDA receptor, plays a role in signal transduction within lipid rafts. In our cell model, knocking-down PrP^C gene impairs ERK phosphorylation induced by tPA and the alteration of the lipidic milieu of lipid rafts inhibits this response perturbing the physical/functional interaction between PrP^C and LRP1.

Taken together, these findings lead to our hypothesis by which, under tPA stimulation, PrP^C and LRP1 associate within a multimolecular complex, also including ganglioside GM1, which is dependent on the integrity of lipid raft and is involved in the neuritogenic signaling and trafficking.

Author contribution

All the Authors conceptualized the research. Va.M. and S.M. performed the experiment. Va.M., S.M., and A.C. contributed to methodology. A.F., T.G. A.C., and A.L. performed the analyses of data. R.M. and V.M. contributed to the writing of the original draft. V.M., R.M., T.G., M.S., A.F., and E.M., contributed to writing the review and editing.

Acknowledgments and conflict of interest disclosure

The authors declare no conflict of interest.

All experiments were conducted in compliance with the ARRIVE guidelines.

Supporting information

Additional supporting information may be found online in the Supporting Information section at the end of the article.

Figure S1. Effect of the raft disrupting agents (MCD or FB1) on the localization of raft/ non-raft markers.

Figure S2. Neurite outgrowth quantification.

Figure S3. Quantification of GAP43 Immunofluorescent staining.

References

Aureli M., Grassi S., Prioni S. and Sonnino S. P. A. (2015) Lipid membrane domains in the brain. *Biochim Biophys Acta* **1851**, 1006–1016.

Barbat C., Trucy M., Sorice M., Garofalo T., Manganelli V. and Fischer A. M. F. (2007) p56lck, LFA-1 and PI3K but not SHP-2 interact with GM1- or GM3-enriched microdomains in a CD4-p56lck association-dependent manner. *Biochem. J.* **402**, 471–481.

Bu G., Maksymovitch E. A., Nerbonne J. M. and Schwartz A. L. (1994) Expression and function of the low density lipoprotein receptor-related protein (LRP) in mammalian central neurons. *J. Biol. Chem.* **269**, 18521–18528.

Cam J. A., Zerbinatti C. V., Li Y. and Bu G. (2005) Rapid endocytosis of the low density lipoprotein receptor related protein modulates cell surface distribution and processing of the beta-amyloid precursor protein. *J. Biol. Chem.* **280**, 15464–15470.

Chen S., Yadav S. P. and Surewicz W. K. (2010) Interaction between human prion protein and amyloid-beta (Abeta) oligomers: role OF N-terminal residues. *Biol. Chem.* **285**, 26377–26383.

De Ferrari G. V., Papassotiropoulos A., Biechele T., et al (2007) Common genetic variation within the low-density lipoprotein receptor-related protein 6 and late-onset Alzheimer's disease. *Proc. Natl Acad. Sci. USA* **104**, 9434–9439.

Dickson R. B., Nicolas J. C., Willingham M. C. and Pastan I. (1981) Internalization of alpha 2 macroglobulin in receptosomes. Studies with monovalent electron microscopic markers. *Exp. Cell Res.* **132**, 488–493.

Echeverry R., Wu J., Haile W. B., Guzman J. and Yepes M. (2010) Tissue-type plasminogen activator is a neuroprotectant in the mouse hippocampus. *J. Clin. Invest.* **120**, 2194–2205.

Ellis V., Daniels M., Misra R. and Brown D. R. (2002) Plasminogen activation is stimulated by prion protein and regulated in a copper-dependent manner. *Biochemistry* **41**, 6891–6896.

Epple G., Langfeld K., Baier M., Holzhutter H. G., Schleuning W. D., Kottgen E., Gessner R. and Praus M. (2004) Both lysine-clusters of the NH2-terminal prion-protein fragment PrP23-110 are essential for t-PA mediated plasminogen activation. *Thromb Haemost* **94**, 465–472.

Fuentealba R. A., Liu Q., Kanekiyo T., Zhang J. and Bu G. (2009) Low density lipoprotein receptor-related protein 1 promotes anti-apoptotic signaling in neurons by activating Akt survival pathway. *J. Biol. Chem.* **284**, 34045–34053.

Garofalo T., Misasi R., Mattei V., Giammarioli A. M., Malorni W., Pontieri G. M., Pavan A. and Sorice M. (2003) Association of the death-inducing signaling complex with microdomains after triggering through CD95/Fas. Evidence for caspase-8-ganglioside interaction in T cells. *J. Biol. Chem.* **278**, 8309–8315.

Gonias S. L. and Campana W. M. (2014) LDL receptor-related protein-1: a regulator of inflammation in atherosclerosis, cancer, and injury to the nervous system. *Am. J. Pathol.* **184**, 18–27.

Gonnord P., Blouin C. M. and Lamaze C. (2012) Membrane trafficking and signaling: two sides of the same coin. *Semin Cell Dev. Biol.* **23**, 154–164.

Hayashi H., Campenot R. B., Vance D. E. and Vance J. E. (2007) Apolipoprotein E-containing lipoproteins protect neurons from apoptosis via a signaling pathway involving low-density lipoprotein receptor-related protein-1. *J. Neurosci.* **27**, 1933–1941.

Herz J. and Chen Y. (2006) Reelin, lipoprotein receptors and synaptic plasticity. *Nat. Rev. Neurosci.* **7**, 850–859.

Hirsch T. Z., Hernandez-Rapp J., Martin-Lannerée S., Launay J. M. and Mouillet-Richard S. (2014) PrP(C) signalling in neurons: from basics to clinical challenges. *Biochimie* **104**, 2–11.

Holtzman D. M., Pitas R. E., Kilbridge J., Nathan B., Mahley R. W., Bu G. and Schwartz A. L. (1995) Low density lipoprotein receptor-related protein mediates apolipoprotein E-dependent neurite outgrowth in a central nervous system-derived neuronal cell line. *Proc. Natl Acad. Sci. USA* **92**, 9480–9484.

Hoylaerts M., Rijken D. C., Lijnen H. R. and Collen D. (1982) Kinetics of the activation of plasminogen by human tissue plasminogen activator. Role of fibrin. *J. Biol. Chem.* **257**, 2912–2919.

Kornblatt J. A., Marchal S., Rezaei H., Kornblatt M. J., Balny C., Lange R., Debey M. P., Hui Bon Hoa G., Marden M. C. and Grosclaude J. (2003) The fate of the prion protein in the prion/plasminogen complex. *Biochem. Biophys Res. Commun.* **305**, 518–522.

Laudati E., Gilder A. S., Lam M. S., Misasi R., Sorice M., Gonias S. L. and Mantuano E. (2016) The activities of LDL Receptor-related Protein-1 (LRP1) compartmentalize into distinct plasma membrane microdomains. *Mol. Cell Neurosci.* **76**, 42–51.

Laurén J., Gimbel D. A., Nygaard H. B., Gilbert J. W. and Strittmatter S. M. (2009) Cellular prion protein mediates impairment of synaptic plasticity by amyloid-beta oligomers. *Nature* **457**, 1128–1132.

Lee S. H., Ko H. M., Kwon K. J., Lee J., Han S. H., Han D. W., Cheong J. H., Ryu J. H. and Shin C. Y. (2014) tPA regulates neurite outgrowth by phosphorylation of LRP5/6 in neural progenitor cells. *Mol. Neurobiol.* **49**, 199–215.

Mantuano E., Lam M. S. and Gonias S. L. (2013) LRP1 assembles unique co-receptor systems to initiate cell signaling in response to tissue-type plasminogen activator and myelin-associated glycoprotein. *J. Biol. Chem.* **288**, 34009–34018.

Mantuano E., Lam M. S., Shibayama M., Campana W. M. and Gonias S. L. (2015) The NMDA receptor functions independently and as an LRP1 co-receptor to promote Schwann cell survival and migration. *J. Cell Sci.* **128**, 3478–3488.

Marasas W. F., Riley R. T., Hendricks K. A., et al (2004) Fumonisins disrupt sphingolipid metabolism, folate transport, and neural tube development in embryo culture and in vivo: a potential risk factor for human neural tube defects among populations consuming fumonisin-contaminated maize. *J. Nutr.* **134**, 711–716.

Martellucci S., Manganelli V., Santacroce C., Santilli F., Piccoli L., Sorice M. and Mattei V. (2018) Role of Prion protein-EGFR multimolecular complex during neuronal differentiation of human dental pulp-derived stem cells. *Prion* **12**, 117–126.

Martellucci S., Santacroce C., Santilli F., Piccoli L., Delle Monache S., Angelucci A., Misasi R., Sorice M. and Mattei V. (2019) Cellular and molecular mechanisms mediated by recPrPC involved in the neuronal differentiation process of mesenchymal stem cells. *Int. J. Mol. Sci.* **20**, E345.

Mattei V., Matarrese P., Garofalo T., et al (2011) Recruitment of cellular prion protein to mitochondrial raft-like microdomains contributes to apoptosis execution. *Mol. Biol. Cell* **22**, 4842–4853.

Mattei V., Santacroce C., Tasciotti V., Martellucci S., Santilli F., Manganelli V., Piccoli L., Misasi R., Sorice M. and Garofalo T. (2015) Role of lipid rafts in neuronal differentiation of dental pulp-derived stem cells. *Exp. Cell Res.* **339**, 231–240.

Mattei V., Martellucci S., Santilli F., Manganelli V., Garofalo T., Candelise N., Caruso A., Sorice M., Scaccianoce S. and Misasi R. (2017) Morphine withdrawal modifies prion protein expression in rat hippocampus. *PLoS ONE* **12**, e0169571.

Mauch D. H., Nägler K., Schumacher S., Göritz C., Müller E. C., Otto A. and Pfrieger F. W. (2001) CNS synaptogenesis promoted by glia-derived cholesterol. *Science* **294**, 1354–1357.

Moestrup S. K., Gliemann J. and Pallesen G. (1992) Distribution of the alpha 2-macroglobulin receptor/low density lipoprotein receptor-related protein in human tissues. *Cell Tissue Res.* **269**, 375–382.

Parkyn C. J., Vermeulen E. G., Mootoosamy R. C., et al (2008) LRP1 controls biosynthetic and endocytic trafficking of neuronal prion protein. *J. Cell Sci.* **121**, 773–783.

Pemberton K., Mersman B. and Xu F. (2018) Using ImageJ to assess neurite outgrowth in mammalian cell cultures: research data quantification exercises in undergraduate neuroscience lab. *J. Undergrad Neurosci Educ.* **16**, A186–A194.

Pietrzik C. U., Busse T., Merriam D. E., Weggen S. and Koo E. H. (2002) The cytoplasmic domain of the LDL receptor-related protein regulates multiple steps in APP processing. *EMBO J.* **21**, 5691–5700.

Pittman R. N., Ivins J. K. and Buettner H. M. (1989) Neuronal plasminogen activators: cell surface binding sites and involvement in neurite outgrowth. *J. Neurosci.* **9**, 4269–4286.

Pizzo P. and Viola A. (2003) Lymphocyte lipid rafts: structure and function. *Curr. Opin. Immunol.* **15**, 255–260.

Praus M., Kettelgerdes G., Baier M., et al (2003) Stimulation of plasminogen activation by recombinant cellular prion protein is conserved in the NH(2)-terminal fragment PrP23- 110. *Thromb Haemost* **89**, 812–819.

Qiu Z., Hyman B. T. and Rebeck G. W. (2004) Apolipoprotein E receptors mediate neurite outgrowth through activation of p44/42 mitogen-activated protein kinase in primary neurons. *J. Biol. Chem.* **279**, 34948–34956.

Roura S., Cal R., Gálvez-Montón C., Revuelta-Lopez E., Nasarre L., Badimon L., Bayes-Genis A. and Llorente-Cortés V. (2014) Inverse relationship between raft LRP1 localization and non-raft ERK1,2/MMP9 activation in idiopathic dilated cardiomyopathy: potential impact in ventricular remodeling. *Int. J. Cardiol.* **176**, 805–814.

Rushworth J. V., Griffiths H. H., Watt N. T. and Hooper N. M. (2013) Prion protein-mediated toxicity of amyloid-β oligomers requires lipid rafts and the transmembrane LRP1. *J. Biol. Chem.* **288**, 8935–8951.

Ryou C., Prusiner S. B. and Legname G. (2003) Cooperative binding of dominant-negative prion protein to kringle domains. *J. Mol. Biol.* **329**, 323–333.

Samson A. L., St Nevin, Croucher D., Niego B., Daniel P. B., Weiss T. W., Moreno E., Monard D., Lawrence D. A. and Medcalf R. L. (2008) Tissue-type plasminogen activator requires a co-receptor to enhance NMDA receptor function. *J. Neurochem.* **107**, 1091–1101.

Schindelin J., Arganda-Carreras I., Frise E., et al (2012) Fiji: an open-source platform for biological-image analysis. *Nat. Methods* **9**, 76–982.

Shi Y., Mantuano E., Inoue G., Campana W. M. and Gonias S. L. (2009) Ligand binding to LRP1 transactivates Trk receptors by a Src family kinase-dependent pathway. *Sci. Signal.* **2**, ra18.

Simons K. and Ikonen E. (1997) Functional rafts in cell membranes. *Nature* **387**, 569–672.

Simons K. and Toomre D. (2000) Lipid rafts and signal transduction. *Nat. Rev. Mol. Cell Biol.* **1**, 31–39.

Sonnino S. and Prinetti A. (2012) Membrane domains and the ''lipid raft'' concept. *Curr. Med. Chem.* **20**, 4–21.

Sorice M., Molinari S., Di Marzio L., Mattei V., Tasciotti V., Ciarlo L., Hiraiwa M., Garofalo T. and Misasi R. (2008) Neurotrophic signalling pathway triggered by prosaposin in PC12 cells occurs through lipid rafts. *Febs J.* **275**, 4903–4912.

Sorice M., Matarrese P., Tinari A., et al (2009) Raft component GD3 associates with tubulin following CD95/Fas ligation. *Faseb J.* **23**, 3298–3308.

Sorice M., Matarrese P., Manganelli V., Tinari A., Giammarioli A. M., Mattei V., Misasi R., Garofalo T. and Malorni W. (2010) Role of GD3-CLIPR-59 association in lymphoblastoid T cell apoptosis triggered by CD95/Fas. *PLoS ONE* **5**, e8567.

Spuch C., Ortolano S. and Navarro C. (2012) LRP-1 and LRP-2 receptors function in the membrane neuron. Trafficking mechanisms and proteolytic processing in Alzheimer's disease. *Front Physiol.* **3**, 269.

Strickland D. K., Gonias S. L. and Argraves W. S. (2002) Diverse roles for the LDL receptor family. *Trends Endocrinol. Metab.* **2**, 66–74.

Taylor D. R. and Hooper N. M. (2006) The prion protein and lipid rafts. *Mol. Membr. Biol.* **23**, 89–99.

Taylor D. R. and Hooper N. M. (2007) The low-density lipoprotein receptor-related protein 1 (LRP1) mediates the endocytosis of the cellular prion protein. *Biochem. J.* **402**, 17–23.

Tsui-Pierchala B. A., Encinas M., Milbrandt J. and Johnson E. (2002) Lipid rafts in neuronal signaling and function. *Trends Neurosci.* **25**, 412–417.

Vetrivel K. S. and Thinakaran G. (2010) Membrane rafts in Alzheimer's disease beta-amyloid production. *Biochim. Biophys Acta.* **1801**, 860–867.

Whitehead S. N., Gangaraju S., Aylsworth A. and Hou S. T. (2012) Membrane raft disruption results in neuritic retraction prior to neuronal death in cortical neurons. *BioScience Trends* **6**, 183–191.

Willingham M. C., Maxfield F. R. and Pastan I. (1980) Receptor-mediated endocytosis of alpha 2-macroglobulin in cultured fibroblasts. *J. Histochem. Cytochem.* **28**, 818–823.

Wu L. and Gonias S. L. (2005) The low-density lipoprotein receptor-related protein-1 associates transiently with lipid rafts. *J. Cell Biochem.* **96**, 1021–1033.

Xanthopoulos K., Paspaltsis I., Apostolidou V., Petrakis S., Siao C. J., Kalpatsanidis A., Grigoriadis N., Tsaftaris A., Tsirka S. E. and Sklaviadis T. (2005) Tissue plasminogen activator in brain tissues infected with transmissible spongiform encephalopathies. *Neurobiol. Dis.* **20**, 519–527.

Yoon I. S., Pietrzik C. U., Kang D. E. and Koo E. H. (2005) Sequences from the low density lipoprotein receptorrelated protein (LRP) cytoplasmic domain enhance amyloid beta protein production via the beta-secretase pathway without altering amyloid precursor protein/LRP nuclear signaling. *J. Biol. Chem.* **280**, 20140–20147.

Yoon I. S., Chen E., Busse T., Repetto E., Lakshmana M. K., Koo E. H. and Kang D. E. (2007) Low-density lipoprotein receptor-related protein promotes amyloid precursor protein trafficking to lipid rafts in the endocytic pathway. *FASEB J.* **21**, 2742–2752.

Zemskov E. A., Mikhailenko I., Strickland D. K. and Belkin A. M. (2007) Cell-surface transglutaminase undergoes internalization and lysosomal degradation: an essential role for LRP1. *J. Cell Sci.* **120**, 3188–3199.

Zerbinatti C. V., Wozniak D. F., Cirrito J., Cam J. A., Osaka H., Bales K. R., Zhuo M., Paul S. M., Holtzman D. M. and Bu G. (2004) Increased soluble amyloid-beta peptide and memory deficits in amyloid model mice overexpressing the low-density lipoprotein receptor-related protein. *Proc. Natl Acad. Sci. USA* **101**, 1075–1080.

Zhuo M., Holtzman D. M., Li Y., Osaka H., DeMaro J., Jacquin M. and Bu G. (2000) Role of tissue plasminogen activator receptor LRP in hippocampal long-term potentiation. *J. Neurosci.* **20**, 542–549.